Nanotechnology **19** (2008) 285301 (6pp) doi:10.1088/0957-4484/19/28/285301

Tunable, high aspect ratio pillars on diverse substrates using copolymer micelle lithography: an interesting platform for applications

S Krishnamoorthy[1], Y Gerbig[1], C Hibert[2], R Pugin[1], C Hinderling[1], J Brugger[2] and H Heinzelmann[1]

[1] Centre Suisse d'Electronique et de Microtechnique SA, Jaquet Droz 1, CH-2007 Neuchâtel, Switzerland
[2] Ecole Polytechnique Fédérale de Lausanne (EPFL), Laboratoire de microsystèmes 1, CH-1015 Lausanne, Switzerland

E-mail: raphael.pugin@csem.ch

Received 26 February 2008, in final form 23 April 2008
Published 2 June 2008
Online at stacks.iop.org/Nano/19/285301

Abstract
We demonstrate the use of copolymer micelle lithography using polystyrene-block-poly(2-vinylpyridine) reverse micelle thin films in their as-coated form to create nanopillars with tunable dimensions and spacing, on different substrates such as silicon, silicon oxide, silicon nitride and quartz. The promise of the approach as a versatile application oriented platform is highlighted by demonstrating its utility for creating super-hydrophobic surfaces, fabrication of nanoporous polymeric membranes, and controlling the areal density of physical vapor deposition derived titanium nitride nanostructures.

1. Introduction

Methods for nanopatterning based on self-assembly have become popular chiefly because they offer the advantage of enabling the patterning of large areas without the need for complex and expensive equipment. While the level of control and perfection as well as the complexity of structures attainable in such bottom up process falls short of what is achievable by top-down methods, there is a very significant area of technology where long-range order is of less concern. Much of the principal requirements for a pattern lie in providing a simple nanostructure with well-controlled size and distance. Structured or patterned surfaces in the nanoscale have been considered for a variety of applications such as influencing cell–substrate interactions [1], catalysis [2], surface adhesion [3], nanoporous MEMS components [4], on-chip microelectronic [5] or lighting [6] devices and biosensing interfaces [7]. Self-assembly of block-copolymeric systems is well suited to cover the range between approximately 10 and 100 nm [8–10]. An interesting use of such nanopatterns is their transfer into hard substrates by dry etching to achieve patterns in nanotopography. This is particularly interesting with materials that are of technological interest in microtechnology or electronics, such as silicon, silicon oxide, silicon nitride and quartz. We demonstrate in this report the use of micelles of block-copolymers as a convenient and effective means of obtaining nanoscale etch masks for the creation of high aspect ratio structures in MEMS compatible substrates [11]. The procedure is based on the use of thin films of block copolymer micelles. Using pre-organized micelles from solution offers several advantages. The micellar films themselves are bumpy and provide the required mass–thickness contrast without the need for any additional processing [12, 13]. The periodicity of the micellar arrays can be tuned in a straightforward manner by simply controlling the deposition conditions. The as-coated micellar films are further responsive and can provide means of achieving complementary nanotopography through exposure to appropriate solvents [12–14].

The use of block-copolymers in the form of microphase-separated thin films have been reported earlier for structuring surfaces [15–21]. Typically, this necessitates additional effort to achieve the required etch-contrast: for example,

by using a special copolymer containing organometallic monomers that result in etch-resistant domains, or by selective chemical degradation of one of the microphase-separated domains. The fabrication of nanoscale pillar arrays using nanospheres [22, 23] or nanoparticles as etch masks [24–27], and through use of anodized alumina as electrodeposition templates [28], has been reported earlier. The nanosphere lithography (NSL) based approach offers complementary advantages compared to the work we have presented here, such as a high mass thickness contrast, shadow-mask profile and feature spacings higher than that possible by molecular self-assembly based methods. Compared to these instances in the literature, the approaches we present benefit from a simplicity in processing, high feature densities and narrow distributions in size and spacing. We demonstrate a simple and flexible procedure that allows creating arrays of pillars with all the structural parameters, namely heights, spacing and to some degree the diameters, continuously tunable in the nanoscale. Tunability is achieved by benefiting from the copolymer self-assembly process itself in addition to varying the reactive-ion etching (RIE) conditions employed for pillar formation. Such high density pillars in silicon based substrates with tunable geometric characteristics in the sub-100 nm scale are of particular interest in applications such as controlling cell–substrate interactions, engineered optical index materials, controlling wettability, cheap stamps for nanoimprint lithography, and as templates for creating or guiding the growth of other nanostructures. We present three such instances where our nanopillar substrates could be put to use: (1) engineered surface wettability, (2) nanoporous freely suspended polymer membranes, and (3) controlling the areal density of physical vapor deposition (PVD) derived titanium nitride (TiN) nanostructures are presented in this context.

2. Fabrication of tunable nanopillar arrays

Two-dimensional (2D) arrays of quasi-hexagonally ordered arrays of polystyrene-block-poly(2-vinylpyridine) (PS-b-P2VP) (91 500-b-105 000 g mol^{-1}, PDI 1.10, Polymer Source Inc. Canada) reverse micelles with a mean spacing of 100 nm were obtained by spin-coating a 0.8% w/v solution of the copolymer in o-xylene at 5000 rpm spin speed. The periodicity of the array on the surface can be tuned in steps of ∼7 nm between 90 and 150 nm by varying either the concentration of the solution between 0.5 and 1 wt% or the spin-coating speeds between 1000 and 10 000 rpm [29]. When the micelles are deposited from solution on to the substrate, they collapse on the surface to form a continuous film due to fusion of the coronal blocks from adjacent micelles. The extent to which the micelles collapse determines the topography exhibited by the resulting film. We have shown earlier that this topography can be enhanced by over 200% by varying the humidity of the spin-coating environment during film formation. Variation in bump heights between 17 and 42 nm is achievable by working between a relative humidity (RH) of 10–60%. For all the lithography experiments presented, the micellar films were coated at 50% RH at 20 °C. The thickness of the mask used for lithography in addition to the selectivity of the dry etching process used eventually determines how deep structures can be obtained and how vertical the resulting features will be. Apart from benefiting from an enhanced topographic contrast by working at higher humidity, we have also derived advantage out of the high selectivity of our dry etch processes. The micelle arrays were coated on different substrates and were exposed to brief oxygen plasma (30 W, 50 mTorr for 25 s using an Oxford Plasmalab 80 Plus, Oxford Instruments, UK) to remove the continuous polymer layer between the bumps and expose the surface beneath. This was followed by dry etching using halogen plasmas to create nanopillars. The experiments were performed using thermal SiO_2, low pressure chemical vapor deposited Si_3N_4, fused quartz and Si(100) as substrates. The dry etching experiments to create nanopillars on SiO_2, Si_3N_4 and quartz were carried out using a dedicated commercial AMS200 inductively coupled plasma (ICP) plasma etcher from Adixen (Alcatel Vacuum Technology, France) using a C_4F_8/CH_4 mixture (10 sccm each) at 6 mTorr pressure, 1500 W ICP power and 120 W substrate-bias. The process yielded an etch rate of 250 nm min^{-1} with a selectivity of 10:1 to polymer masks. Helium gas (150 sccm) was used as a diluent to control the gas residence times and achieve better anisotropy. Etching in the case of these substrates is facilitated through a highly ion assisted bombardment process. The average ion energy is controlled with the substrate holder voltage biasing by applying radiofrequency (RF) power (13.56 MHz). The key parameters to achieve a high selectivity process are an optimum C_4F_8/CH_4 gas mixture (C/F ratio), ICP power, pressure and substrate-bias. The dry etching of Si is a more chemically assisted process and was carried out using SF_6/C_4F_8 gas mixture (SF_6: 60 sccm, C_4F_8: 40 sccm) at 10 mTorr pressure, and substrate-bias of 100 W. Under these conditions, the process was capable of providing an etch rate of 0.6–1.5 μm (depending on the Si load) with a selectivity of 20:1 towards the SiO_2 mask. The fabrication of silicon nanopillars using a chlorine based plasma was carried out in an STS multiplex ICP etcher (Surface Technology Systems, UK) with an ICP power of 1000 W, substrate-bias of 100 W, 5 mTorr pressure, and 10 sccm flow of chlorine gas, offering an etch rate of 350 nm min^{-1} with a selectivity of 8:1 towards the SiO_2 mask.

There were two different processes that were employed for creating nanopillars. In the first process, micelle arrays that were coated on SiO_2, Si_3N_4 or quartz substrates were subjected to brief oxygen plasma to expose the surface between the bumps. In the subsequent step, the polymer masks were transferred into the substrate using C_4F_8/CH_4 plasma, to obtain the corresponding nanopillars (figures 1(a), (b)). Any polymer left behind is removed using an oxygen plasma exposure at the end. The fluorine plasma exposure time can further be varied to control the pillar aspect ratios (figure 1(c)) and the periodicities of pillar arrays can be varied by starting with micelle arrays of different periodicities (figure 1(d)). In the second process, micelles were coated on silicon substrates consisting of thermally grown SiO_2 layers of 25 nm thickness. The micelle structures, after the brief O_2 plasma pre-treatment, are first transferred into the SiO_2 intermediate layer to create SiO_2 particle masks using C_4F_8/CH_4 plasma. The SiO_2 mask is subsequently transferred into Si in the next step by means of

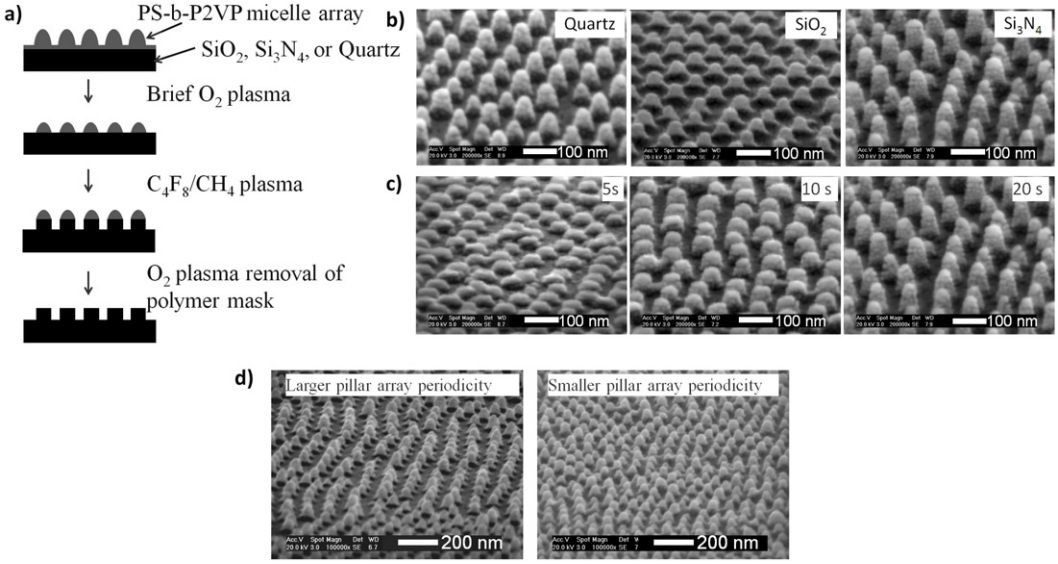

Figure 1. (a) Scheme presenting the process steps used for transferring PS-b-P2VP micelle array patterns into SiO_2, Si_3N_4 and quartz substrates. SEM images of nanopillars on (b) the indicated substrates, with (c) tunable aspect ratios (shown are Si_3N_4 pillars; the duration of plasma etching is indicated) and (d) tunable array periodicities (shown are SiO_2 pillars).

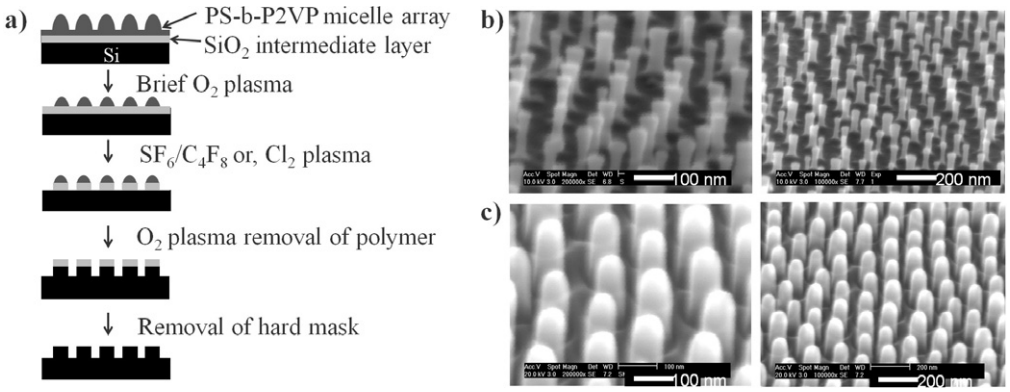

Figure 2. (a) Scheme presenting the process steps used for transferring PS-b-P2VP micelle array patterns into Si, mediated by a first transfer into an intermediate SiO_2 thin film. (b), (c) SEM images of Si pillars etched using (b) SF_6/C_4F_8 and (c) Cl_2 plasma.

SF_6/C_4F_8 plasma or Cl_2 plasma (figure 2(a)). The SiO_2 mask is finally stripped off using a 5% HF aqueous solution to obtain Si pillar arrays (figures 2(b), (c)). The use of an intermediate SiO_2 hard mask helps overcome the mask limitations to achieve high aspect ratios [30]. The advantage was gained from the process conditions that offered high selectivity to SiO_2. When only the polymer mask was used, without an intermediate layer, the aspect ratios were limited mainly by the mask erosion. Also, the shape of the pillars resembles the mask profile as a result. Thus, in the case of SiO_2, Si_3N_4 and quartz substrates where only polymer masks were used for structuring, the pillars exhibit a convex profile due to the mask erosion. It can be observed, however, that the Si pillars are far more vertical in comparison, which could be attributed to the resistance offered by SiO_2 masks to erosion.

An attractive means of tuning pillar diameters arises from controlling the diameter of the polymer mask obtained upon oxygen plasma exposure of the as-coated micelle arrays. The polymer masks are convex shaped and the diameter of the masks formed can be controlled by varying the oxygen plasma exposure duration. Higher exposure durations lead to smaller polymer mask diameters, which results in thinner pillars in the end. Si pillars etched using polymer masks that were obtained after 25 and 50 s of oxygen plasma exposure of the as-coated PS-b-P2VP micelle arrays are shown in figure 3. In three different durations of exposure (0 s, 25 s, and 50 s of oxygen plasma) pillars of diameters of 80, 40 and 20 nm could be achieved. This offers some degree of freedom towards controlling the pillar diameters independent of the micelle dimensions.

3. Applying nanopillar arrays

3.1. Engineered surface wettability

We have shown the use of these pillars for three different applications (figure 4). The first is the substantial reduction in

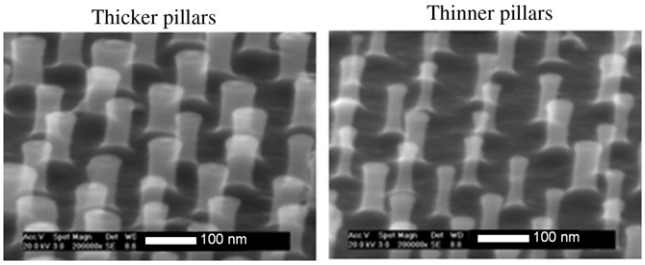

Figure 3. SEM images showing Si pillars with (left) larger and (right) smaller mean diameters obtained by starting from PS-b-P2VP micelle arrays that have been exposed to 25 and 50 s oxygen plasma exposures respectively.

surface wettability benefiting from surface roughness induced enhancement in hydrophobicity. Figure 4(a) shows static water droplet profiles on a flat Si_3N_4 substrate and Si_3N_4 surface structured with 70 nm high pillars and 100 nm periodicity. Both the substrates were silanized with perfluorosilane (1H, 1H, 2H, 2H- perfluorooctyldimethylchlorosilane, Gelest, UK), through vapor phase exposure of oxygen plasma pre-treated substrates for a duration of 2 h. The contact angle increases from 111° on the flat surface to 150° in the case of the pillar substrate. The influence of surface roughness on wettability has been discussed in several earlier works [31–35]. What we present here is a means of achieving periodic surface roughness with tunable geometric characteristics over large areas. Also, the wetting behavior on rough surfaces based on the Cassie and Wenzel theories have shown to be controllable by varying the characteristics of the rough surface. Optimizing the geometric characteristics of surface roughness is understood to be essential in order to create 'robust' super-hydrophobic surfaces. In the case of periodic surfaces the wetting behavior can be varied between the Cassie and Wenzel regimes by varying the aspect ratios as well as the periodicity of the nanopillars [36, 37]. The equations predicting the apparent water contact angle (θ) based on Wenzel and Cassie theories, for a hexagonal lattice of cylindrical pillars (height: h, radius: r, periodicity: a) can be derived to be

$$\theta_{\text{Wenzel}}(h, r, a) = a\cos\left[\left(1 + \frac{4\pi rh}{\sqrt{3}a^2}\right)\cos\theta_{\text{flat}}\right]\frac{180}{\pi}$$

$$\theta_{\text{Cassie}}(r, a) = a\cos\left[2r^2\frac{\pi}{\sqrt{3}a^2}(\cos\theta_{\text{flat}} + 1) - 1\right]\frac{180}{\pi}.$$

In our case, assuming a cylindrical morphology for the silicon nitride pillars and using experimentally determined values for $r = 20$ nm, $h = 70$ nm, $a = 100$ nm and $\theta_{\text{flat}} = 111°$ respectively, $\theta_{\text{Cassie}} = 155°$ and $\theta_{\text{Wenzel}} = 133°$ can be obtained. The surface in this case could hence be behaving the Cassie way rather than the Wenzel way. Thus our pillar substrates offer potential as excellent model surfaces for studying the wetting phenomena, as the values for h, r and a can be varied systematically. Shiu *et al* have earlier shown the use of colloidal lithography derived tunable patterning to influence surface wettability [35]. The approach suffers from the disadvantage that only the height and the radius of features can be varied, while the spacing remains constant. The structuring in our case presents far higher feature densities and facile tunability in spacing, and thus serves a promising means towards the design and engineering of robust super-hydrophobic surfaces.

3.2. Nanoporous freely suspended polymer membranes

In the second example, we present the use of the pillar substrates as templates to create nanoporous PMMA membranes (figure 4(b)). A 2% w/v solution of PMMA was spin-coated on a SiO_2 pillar substrate at 3000 rpm. The pillars had a mean height of ∼70 nm. The pillar substrate with PMMA film on top was annealed at 200 °C for 20 min to enable flow of polymer from the top of the pillars and to ensure homogeneity. A short oxygen plasma exposure (30 W, 50 mTorr, 15 s) was carried out to remove any polymer remaining on the top of the pillars. The substrate was dipped in HF to dissolve the pillars and lift off the porous PMMA film. The free-floated film was picked up with a transmission electron microscopy (TEM) grid. The scanning electron microscopy (SEM) characterization was carried out on

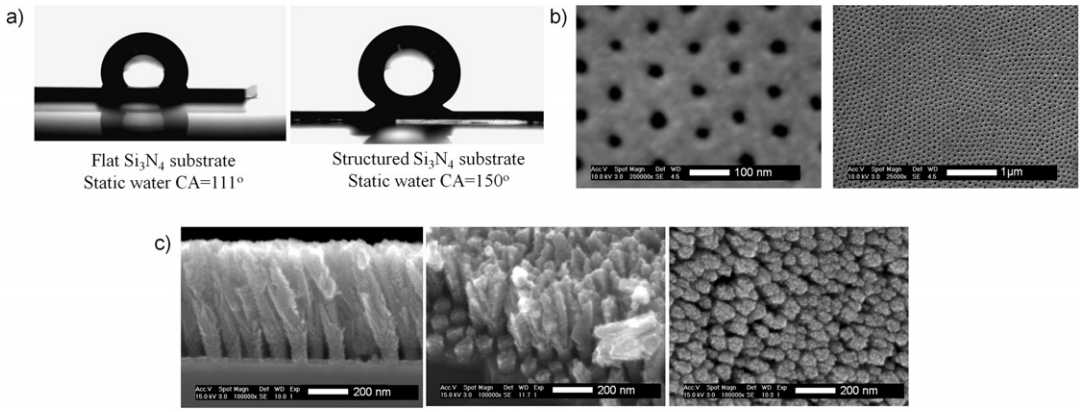

Figure 4. Three examples where the pillar substrates were applied are presented. (a) Optical pictures of water droplet profiles on flat and structured Si_3N_4 substrates; the surfaces have been pre-treated with perfluoro silane. (b) SEM images of nanoporous PMMA films supported on a TEM grid obtained using SiO_2 nanopillars as templates. (c) SEM images of titanium nitride pyramids grown using physical vapor deposition, on Si_3N_4 nanopillars. Selective growth of the TiN pyramids on the top of pillars can be seen.

the TEM grid supported nanoporous PMMA membrane after sputtering 5 nm of Au to counter the charging effects. The technique can easily be extended to a variety of other polymers and opens up opportunities for applications that would benefit from the tunability in size of the pores, the periodicity and thickness. Creating nanoporous templates on surfaces have been shown earlier in relevance to etching holes using block copolymer lithography [14, 38–40]. These processes suffer from the disadvantage that the template obtained depends on the block copolymer system used (block ratios, possibility for selective degradation of the other domain, etc). Also, the use of a freely supported nanoporous template that we have presented can enable 'reusability' in addition to extending its utility for other applications such as stencil membranes. Although the technique we have presented has the drawback of having to sacrifice the SiO_2 nanopillar substrate, conditions can in principle be optimized to facilitate the lifting off of the porous mask without etching the pillars, but by controlling the polarity of the substrate and the lift-off solvent.

3.3. Controlling growth density of PVD grown TiN nanopyramids

In yet another instance, we present the use of silicon nitride pillar arrays as templates to control the growth density of TiN nanopyramids. TiN coatings are sought after for medical implant applications for the high degree of bioactivity they exhibit in addition to remarkable corrosion and wear resistance [41–43]. These coatings also hold promise for use in microelectronic applications owing to the high conductivity and excellent performance as an adhesion layer [44]. The titanium nitride films were deposited by RF sputtering in a home-built PVD unit. In a stainless steel reactor chamber (volume $\sim$ 0.04 m^3), three cathodes (targets) are installed above the table (bottom electrode) on which the samples are placed. The target–sample distance is $\sim$6 cm. The cathodes are connected with a DC magnetron power supply. The pumping system of this PVD unit consists of a turbomolecular pump in series with a rotary vane pump. Prior to deposition the deposition chamber was evacuated to a base pressure of 0.005 Pa and then backfilled with argon to obtain a total pressure of 1 Pa. The samples were coated by operating the TiN target for 60 min at 150 W sputter power. No bias was applied at the substrate table during the deposition.

The results show a lower density of TiN crystals on the nanostructured surfaces. About three pyramids were found to be growing from the top of each of the Si_3N_4 pillars (figure 4(c)). Pyramidal surface features obtained from the PVD growth are due to the (111) orientation of the TiN crystals [43]. The open, columnar microstructure of this topography type is caused by the limited surface diffusion under conditions of relatively low deposition temperatures and low ion energy (bias voltages) of the deposition process [45, 46]. It would be possible to obtain single TiN pyramids per nanopillar by adjusting the geometry of the pillars, mainly the aspect ratio. Nanostructured surfaces such as those obtained in the case of TiN coatings discussed above have been known to influence cell adhesion and expression [47, 48]. Controlling the density of nanostructures such as presented here provides a promising way towards optimizing the surface to invoke an appropriate cell response.

4. Conclusions

We have thus presented a means of fabricating high density nanopillar arrays on large areas of the surface starting from copolymer micelle self-assembly on different silicon based surfaces. The approach clearly benefits from the ease and economy of processing in comparison to the use of other self-assembly based approaches such as copolymer phase-separated thin films, or nanosphere lithography. We highlight that the tunability in the pillar dimensions and spacing shown here has been achieved without having to change the polymer, and simply by varying the coating and etching conditions. Further, the process is fairly independent of the surface topography and surface energy which phase-separated copolymer thin films are sensitive to. Some applications of the nanopillar substrates which specially benefit from the tunability aspects presented in the paper have been presented to bring out the significance of the approach and its promise as a versatile technology platform.

Acknowledgments

This work has been supported by the European Commission through the Sixth Framework Program for Research and Technological Development with up to 11.7 million Euros, with the NAPOLYDE project, NMP2-CT-2005-515846, which addresses the NMP thematic area 'Nanotechnologies and nanosciences, knowledge based multifunctional materials and new production processes and devices'. The authors thank NCCR nanoscale science for partial support. The authors also thank the technical staff of the CSEM/IMT common lab COMLAB for their support in preparing silicon oxide and silicon nitride coatings and for the instrument facility for characterization. Helpful discussions with Dr A Hoogerwerf, CSEM SA, were highly appreciated.

References

[1] Arnold M *et al* 2004 *ChemPhysChem* **5** 383
[2] Hinderling C *et al* 2004 *Adv. Mater.* **16** 876
[3] Geim A K, Dubonos S V, Grigorieva I V, Novoselov K S, Zhukov A A and Shapoval S Y 2003 *Nat. Mater.* **2** 461
[4] Hoogerwerf A C, Hinderling C, Krishnamoorthy S, Hibert C, Spassov V and Overstolz T 2007 *Solid-State Sensors, Actuators and Microsystems Conf. TRANSDUCERS 2007 International* p 489
[5] Black C T *et al* 2007 *IBM J. Res. Dev.* **51** 605
[6] Linn N C, Sun C H, Jiang P and Jiang B 2007 *Appl. Phys. Lett.* **91** 101108
[7] Cai Y and Ocko B M 2005 *Langmuir* **21** 9274
[8] Fasolka M J and Mayes A M 2001 *Annu. Rev. Mater. Res.* **31** 323
[9] Lazzari M and Lopez-Quintela M A 2003 *Adv. Mater.* **15** 1583
[10] Park C, Yoon J and Thomas E L 2003 *Polymer* **44** 6725
[11] Riess G 2003 *Prog. Polym. Sci.* **28** 1107

[12] Meiners J C, Ritzi A, Rafailovich M H, Sokolov J, Mlynek J and Krausch G 1995 *Appl. Phys.* A **61** 519
[13] Meiners J C, Elbs H, Ritzi A, Mlynek J and Krausch G 1996 *J. Appl. Phys.* **80** 2224
[14] Krishnamoorthy S, Pugin R, Brugger J, Heinzelmann H, Hoogerwerf A C and Hinderling C 2006 *Langmuir* **22** 3450
[15] Park M, Harrison C, Chaikin P M, Register R A and Adamson D H 1997 *Science* **276** 1401
[16] Harrison C, Park M, Chaikin P M, Register R A and Adamson D H 1998 *J. Vac. Sci. Technol.* B **16** 544
[17] Li R R, Dapkus P D, Thompson M E, Jeong W G, Harrison C, Chaikin P M, Register R A and Adamson D H 2000 *Appl. Phys. Lett.* **76** 1689
[18] Cheng J Y, Ross C A, Chan V Z H, Thomas E L, Lammertink R G H and Vancso G J 2001 *Adv. Mater.* **13** 1174
[19] Lammertink R G H, Hempenius M A, Thomas E L and Vancso G J 1999 *J. Polym. Sci.* B **37** 1009
[20] Lammertink R G H, Hempenius M A, Chan V Z H, Thomas E L and Vancso G J 2001 *Chem. Mater.* **13** 429
[21] Hempenius M A, Lammertink R G H, Peter M and Vancso G J 2003 *Macromol. Symp.* **196** 45
[22] Manzke A *et al* 2007 *Adv. Mater.* **19** 1337
[23] Sinitskii A, Neumeier S, Nelles J, Fischler M and Simon U 2007 *Nanotechnology* **18** 305307
[24] Kuo C W, Shiu J Y and Chen P 2003 *Chem. Mater.* **15** 2917
[25] Rafiq M A, Mizuta H, Uno S and Durrani Z A K 2007 *Microelectron. Eng.* **84** 1515
[26] Lin G R, Lin C J and Kuo H C 2007 *Appl. Phys. Lett.* **91** 093122
[27] Sainiemi L *et al* 2007 *Nanotechnology* **18** 505303
[28] Kouklin N A and Liang J 2006 *J. Electron. Mater.* **35** 1133
[29] Krishnamoorthy S, Pugin R, Liley M, Heinzelmann H, Brugger J and Hinderling C 2006 *Adv. Funct. Mater.* **16** 1469
[30] Guarini K W, Black C T, Zhang Y, Kim H, Sikorski E M and Babich I V 2002 *J. Vac. Sci. Technol.* B **20** 2788
[31] He B, Patankar N A and Lee J 2003 *Langmuir* **19** 4999
[32] Patankar N A 2003 *Langmuir* **19** 1249
[33] He B, Lee J and Patankar N A 2004 *Colloids Surf.* A **248** 101
[34] Chen Y, He B, Lee J and Patankar N A 2005 *J. Colloid Interface Sci.* **281** 458
[35] Shiu J Y, Kuo C W, Chen P L and Mou C Y 2004 *Chem. Mater.* **16** 561
[36] Cassie A B D and Baxter S 1945 *Nature* **155** 21
[37] Wenzel R N 1949 *J. Phys. Colloid Chem.* **53** 1466
[38] Xu T *et al* 2003 *Adv. Funct. Mater.* **13** 698
[39] Black C T, Guarini K W, Milkove K R, Baker S M, Russell T P and Tuominen M T 2001 *Appl. Phys. Lett.* **79** 409
[40] Guarini K W, Black C T, Milkove K R and Sandstrom R L 2001 *J. Vac. Sci. Technol.* B **19** 2784
[41] Piscanec S *et al* 2004 *Acta Mater.* **52** 1237
[42] Burmeister F, Kohn C, Kuebler R, Kleer G, Blasi B and Gombert A 2005 *Surf. Coat. Technol.* **200** 1555
[43] Burmeister F, Schaffer E, Kleer G, Doll W, Blasi B and Gombert A 2005 *Surf. Coat. Technol.* **200** 1088
[44] Wittmer M 1985 *J. Vac. Sci. Technol.* A **3** 1797
[45] Thornton J A 1977 *Annu. Rev. Mater. Sci.* **7** 239
[46] Petrov I, Barna P B, Hultman L and Greene J E 2003 *J. Vac. Sci. Technol.* A **21** S117–28
[47] Cyster L A, Parker K G, Parker T L and Grant D M 2004 *Biomaterials* **25** 97
[48] Manso M, Ogueta S, Perez-Rigueiro J, Garcia J P and Martinez-Duart J M 2002 *Biomol. Eng.* **19** 239